



1 **Spatial and seasonal variability in volatile organic sulfur**  
2 **compounds in seawater and overlying atmosphere of the Bohai**  
3 **and Yellow Seas**

4 **Juan Yu<sup>1,2,3,†</sup>, Lei Yu<sup>1,†</sup>, Zhen He<sup>1,2,3</sup>, Gui-Peng Yang<sup>1,2,3,\*</sup>, Jing-Guang Lai<sup>1</sup>, Qian Liu<sup>1</sup>**

5 <sup>1</sup>Frontiers Science Center for Deep Ocean Multispheres and Earth System, Key Laboratory of Marine Chemistry  
6 Theory and Technology, Ministry of Education, Ocean University of China, Qingdao 266100, China.

7 <sup>2</sup>Laboratory for Marine Ecology and Environmental Science, Qingdao National Laboratory for Marine Science and  
8 Technology, Qingdao 266237, China.

9 <sup>3</sup>Institute of Marine Chemistry, Ocean University of China, Qingdao 266100, China.

10

11 **Abstract.** To better understand the production and loss processes of volatile organic sulfur compounds (VSCs) and  
12 their influence factors, VSCs including carbon disulfide (CS<sub>2</sub>), dimethyl sulfide (DMS), and carbonyl sulfide (COS)  
13 were surveyed in the seawater and atmosphere of the Bohai and Yellow Seas during spring and summer of 2018. The  
14 concentration ranges of COS, DMS, and CS<sub>2</sub> in the surface seawater during spring were 0.14–0.42, 0.41–7.74, and  
15 0.01–0.18 nmol L<sup>-1</sup>, respectively, and 0.32–0.61, 1.31–18.12, and 0.01–0.65 nmol L<sup>-1</sup> during summer. COS and CS<sub>2</sub>  
16 had high concentrations in coastal waters, which may be due to elevated photochemical production rates. High DMS  
17 concentrations occurred near the Yellow River, Laizhou Bay, and Yangtze River Estuary coinciding with high nitrate  
18 and Chl *a* concentrations due to river discharge during summer. The depth distributions of COS, DMS, and CS<sub>2</sub> were  
19 characterized by high concentrations in the surface seawater that decreased with depth. The mixing ratios of COS,  
20 DMS, and CS<sub>2</sub> in the atmosphere were 255.9–620.2 pptv, 1.3–191.2 pptv, and 5.2–698.8 pptv during spring, and

---

\* Corresponding author at: Key Laboratory of Marine Chemistry Theory and Technology, Ministry of Education, Ocean University of China, 238 Songling Road, Qingdao 266100, China. E-mail address: gpyang@mail.ouc.edu.cn (G.-P. Yang)

†These authors contributed equally to this work and should be considered co-first authors.



21 394.6–850.1 pptv, 10.3–464.3 pptv, and 15.3–672.7 pptv in summer. The mean oceanic/atmospheric concentrations  
22 of COS, DMS, and CS<sub>2</sub> were 1.8/1.7-, 3.1/4.7-, and 3.7/1.6-fold higher in summer than spring due to the high Chl *a*  
23 concentrations in summer. The mean sea-to-air fluxes of COS, DMS, and CS<sub>2</sub> were 1.3-, 2.1-, and 3.0-fold higher in  
24 summer than spring. The sea-to-air fluxes of VSCs indicated that these marginal seas are major sources of VSCs in  
25 the atmosphere. The results provide help with a better understanding of the control of VSCs distributions in marginal  
26 seas.

27 **Keywords:** Volatile organic sulfur compound; Carbonyl sulfide; Dimethyl sulfide; Carbon disulfide



## 28 **1 Introduction**

29 Carbonyl sulfide (COS), dimethyl sulfide (DMS), and carbon disulfide (CS<sub>2</sub>) are three major volatile organic sulfur  
30 compounds (VSCs) in seawater and the marine atmosphere and their biogeochemical cycles are closely related to  
31 climate change (Charlson et al., 1987; Li et al., 2022). VSCs are important in the formation of atmospheric cloud  
32 condensation nuclei (CCN) and sulfate aerosols, which have significant implications in the global radiation budget  
33 and ozone concentration (Andreae and Crutzen, 1997). COS can be converted to sulfate aerosols in the stratosphere  
34 and affect Earth's radiation balance (Crutzen, 1976). Atmospheric DMS can react with OH and NO<sub>3</sub> radicals to form  
35 SO<sub>2</sub> and methane sulfonic acid (MSA, CH<sub>3</sub>SO<sub>3</sub>H), and then form non-sea salt sulfates (nss-SO<sub>4</sub><sup>2-</sup>), all of which  
36 contribute to acid deposition and CCN (Charlson et al., 1987). CS<sub>2</sub> is the key precursor of COS and 82% COS is the  
37 oxidation production of CS<sub>2</sub> (Lennartz et al., 2020). Hence, interest in the distribution, production, and chemistry of  
38 VSCs has grown in recent years (Lennartz et al., 2017; Lennartz et al., 2020; Li et al., 2022; Remaud et al., 2022;  
39 Whelan et al., 2018; Yang et al., 2008; Yu et al., 2022). Some researches indicates that the ocean is the source of VSCs  
40 (Chin and Davis, 1993; Yu et al., 2022). Opposite results also were reported that the ocean is the sink of VSCs (Zhu  
41 et al., 2019).

42 COS, with an average tropospheric residence time of 2–7 years, is the most abundant and widely distributed reduced  
43 sulfur trace gas in the atmosphere (Brühl et al., 2012). Atmospheric COS is mainly directly originated from oceanic  
44 emissions and indirectly from oxidations of dimethylsulfide (DMS) and carbon disulfide (CS<sub>2</sub>) (Kettle et al., 2002;  
45 Lennartz et al., 2020). Uptake by terrestrial vegetation and soil is the most important sink of atmospheric COS (Kettle  
46 et al., 2002; Maignan et al., 2021). Therefore, COS is recognized as a proxy for estimating the photosynthesis rate in  
47 ecosystems (Campbell et al., 2008). DMS is the predominant biogenic sulfur originated from  
48 dimethylsulfoniopropionate (DMSP) which is mainly produced by bacteria and phytoplankton (Curson et al., 2017;  
49 Keller et al., 1989). Community composition of phytoplankton and bacteria can affect the net DMSP concentrations  
50 via synthesis and degradation (O'Brien et al., 2022, Zhao et al., 2021). DMS entering the atmosphere via sea-to-air  
51 exchange accounts for about 50% of all natural sulfur release (Cline and Bates, 1983). Photochemical reaction with  
52 dissolved organic matter is a principal source of CS<sub>2</sub> in seawater (Xie et al., 1998). The anthropogenic CS<sub>2</sub> source  
53 were rayon and/or aluminum production, fuel combustion, oil refineries, and coal combustion (Campbell et al., 2015;  
54 Zumkehr et al., 2018). Two different approaches (ice core (Aydin et al., 2020) and isotope measurements (Hattori et



55 al., 2020)) were used to evaluate anthropogenic COS emissions. The latter study and a modeling approach used by  
56 Remaud et al. (2022) all found the gradient of anthropogenic COS in East Asia. Anthropogenic COS is initially emitted  
57 as CS<sub>2</sub> and oxidized by OH to COS in the atmosphere (Kettle et al., 2002). The production and loss of VSCs involves  
58 in phytoplankton and bacteria synthesis, zooplankton grazing, bacterial degradation, sea-air diffusion, photo-oxidation  
59 and/or photochemical reaction (Schäfer et al., 2010). The mechanisms of production and loss processes still need to  
60 be declared.

61 Yu et al. (2022) investigated the distributions of COS, DMS, and CS<sub>2</sub> and sea-to-air flux in Changjiang Estuary and  
62 its adjacent East China Sea and showed that the oceanic VSCs (COS, DMS, and CS<sub>2</sub>) are sources of atmospheric  
63 VSCs. Different from Yu et al. (2022), Zhu et al. (2019) showed that the ocean is a sink for COS. The YS and BS are  
64 semi-enclosed seas of the northwestern Pacific Ocean, the hydrological characteristics of this area are greatly affected  
65 the BS coastal current, YS coastal current, and YS warm current (Chen, 2009), which may alter the VSCs distributions  
66 via exchanges of water mass. In addition, the Yellow Sea Cold Water Mass (YSCWM), a seasonal hydrological  
67 phenomenon, located in the 35°N transect forms, peaks, and disappears in spring, summer, and after September,  
68 respectively (Zhang et al., 2014). In this study, we investigate the spatial distributions and seasonal variability of COS,  
69 DMS, and CS<sub>2</sub> in the seawater and overlying atmosphere of the Yellow Sea (YS) and Bohai Sea (BS) and the effects  
70 of YSCWM on VSCs distributions to better understand the production and loss processes of VSCs.

## 71 **2 Materials and methods**

### 72 **2.1 Sampling**

73 Two cruises were conducted aboard the R/V “Dong Fang Hong 2” in the YS and BS from 28 March to 16 April  
74 (spring) 2018 and from 24 July to 8 August (summer) 2018. The sampling stations are shown in Fig. 1. Seawater  
75 samples were collected using 12 L Niskin bottles mounted on a Seabird 911 CTD (conductivity-temperature-depth)  
76 rosette. The seawater was slowly siphoned from the Niskin bottles into 100 mL glass jaw bottles (CNW Technologies  
77 GmbH, GER) via a translucent silicone tube. The seawater was allowed to overflow the sampling bottle by twice its  
78 volume before the silicone tube was gently removed and the bottle was immediately sealed with an aluminum cap  
79 containing a Teflon-lined butyl rubber septum without any headspace. After seawater the samples were collected, the  
80 concentrations of oceanic VSCs were immediately measured on the ship. The environmental and hydrological



81 parameters such as seawater temperature and salinity were measured simultaneously by the CTD equipment.

82 Atmospheric samples were collected using cleaned and vacuumed SilcoCan canisters (Restek, USA) placed where  
83 atmospheric VSCs were collected in the windward direction approximately 10 m above the ocean. The stability of  
84 VSCs in this kind of fused silica-lined canister has been verified by previous studies (Brown et al., 2015). Brown et  
85 al. (2015) verified the stability of VSCs during storage for 16 d at room temperature. The atmospheric samples were  
86 analyzed immediately after being brought back to the laboratory.

## 87 **2.2 Analytical procedures**

88 VSCs in seawater were measured using a gas chromatographer (GC) (Agilent 7890A, USA) with a flame photometric  
89 detector (FPD) and atmospheric VSCs were measured using a GC equipped with mass spectrometric detector (GC-  
90 MSD) (Agilent 7890A/5975C, USA) according to the methods of Inomata et al. (2006) and Staubes and Georgii  
91 (1993), respectively. A CP-Sil 5 CB column (30 m × 0.32 mm × 4.0 μm, Agilent Technologies, USA) was used to  
92 separate the three VSCs. A standard curve was performed by measuring different concentrations of standard VSC  
93 gases (COS, DMS, and CS<sub>2</sub> mixing ratios were 1 pptv, Beijing Minnick Analytical Instrument Equipment Center).  
94 Qualitative analysis was conducted via comparison with the retention times of the standards, while quantitative  
95 analysis was conducted by diluting the VSC standard gases to specific concentrations using the 2202A dynamic  
96 dilution meter (Nutech, USA) and then injecting different volumes of the diluted VSC standards into the GC using a  
97 gas-tight syringe. The VSC standard gases were used to provide a range of different concentrations and peak areas.  
98 Based on the similarities between the concentrations and the peak areas of the standards and samples, the  
99 concentrations of VSCs in the samples were obtained.

100 The concentrations of VSCs in seawater were determined using a cryogenic purge-and-trap system coupled with  
101 the GC-FPD. A 30 mL seawater sample was injected into glass bubbling chamber by a gas tight syringe (SGE,  
102 Australia). The VSCs were stripped from the seawater with high purity N<sub>2</sub> at a rate of 60 mL min<sup>-1</sup> for 15 min and  
103 passed through an anhydrous CaCl<sub>2</sub>-filled drying tube and a 100% degreasing cotton-filled 1/4 Teflon tube to remove  
104 water and oxides. After that, the VSCs gases were passed through a six-way valve and trapped in a loop of a 1/16  
105 Teflon capture tube immersed in liquid nitrogen. When the VSCs were all purged from the seawater, the capture tube  
106 was removed from the liquid nitrogen and placed it into hot water (> 90 °C) to desorb the trapped VSCs. At the same



107 time, VSCs gases were carried into the GC by N<sub>2</sub> and then detected by the FPD. The column temperature was  
108 programmed with an initial temperature of 55 °C, followed by an increase to 100 °C at 10 °C min<sup>-1</sup>, and a final increase  
109 to 150 °C at 15 °C min<sup>-1</sup>. The inlet and detector temperatures were 150 °C and 160 °C, respectively, and the split ratio  
110 of pure N<sub>2</sub> was 10:1. The detection limit of the method for VSCs was 2.5~3.5 ng and the measurement precision was  
111 3.2%~5.1% (Zhu et al., 2017).

112 The concentrations of atmospheric VSCs were analyzed using an Entech 7100 pre-concentrator (Nutech, USA)  
113 coupled with the GC-MSD. A sampled SilcoCan canister was connected to the pre-concentrator and 200 mL of gas  
114 was drawn into the preconcentration system with a three-stage cold trap. The pre-concentrator parameters of three-  
115 stage cold trap are shown in Table S1. The first trap removes the N<sub>2</sub>, O<sub>2</sub>, and H<sub>2</sub>O (g) from the atmospheric samples  
116 and the second trap eliminates the CO<sub>2</sub>. As for the third trap, it is necessary to obtain the better peak shapes and  
117 separation of the three VSCs. The temperature programming of the column was the same as for the seawater samples.  
118 In addition, the temperature of the quadrupole and ion source were 110 °C and 230 °C, respectively, and the electron  
119 ionization source was run at 70 eV. The carrier gas had a split ratio of 10:1 and a flow rate of 2.0 mL min<sup>-1</sup>. Qualitative  
120 and quantitative analysis of the VSCs was tested using the full scan mode (SCAN) and the selected ion monitoring  
121 mode (SIM). The detection limit of the method for VSCs was 0.1~0.5 pptv (Zhu et al., 2017).

### 122 **2.3 Calculation of VSCs sea-to-air flux**

123 To estimate the VSCs volatilization from ocean to atmosphere, the sea-to-air fluxes of the VSCs were calculated  
124 according to the model established by Liss and Slater (1974) with the following equation:  $F = k_w(c_w - c_g/H)$ , where  $F$  is  
125 the sea-to-air flux of VSCs ( $\mu\text{mol m}^{-2} \text{d}^{-1}$ );  $k_w$  is the VSCs transfer velocity ( $\text{m d}^{-1}$ );  $c_w$  and  $c_g$  are the equilibrium  
126 concentrations of VSCs in the surface seawater and the atmosphere ( $\text{nmol L}^{-1}$ ), respectively; and  $H$  is the Henry's  
127 constant calculated using the formula found in Table S2, which is converted to a dimensionless constant using the  
128 conversion formula constructed by Sander (2015).  $k_w$  was calculated by the N2000 method (Nightingale et al., 2000),  
129 which has been internationally accepted, and the specific calculation introduced by Kettle et al. (2001).

### 130 **2.4 Nitrate, Chl a and dissolved organic carbon (DOC) measurement**

131 Seawater were filtered through Whatman GF/F filters (0.7  $\mu\text{m}$ ), and then the filtered water samples were stored at  
132 -20 °C before nitrate analysis. A continuous flow analyzer (Skalar Analytical, Breda, Netherlands) were used to



133 measure nitrate concentrations. Chl *a* were extracted with 90% acetone for 24 h at 4 °C in darkness. Chl *a*  
134 concentrations were determined following the method of Parsons et al. (1984) with a fluorescence  
135 spectrophotometer (F-4500, Hitachi). Nitrate and Chl *a* data were provided by open research cruise supported by  
136 NSFC Shiptime Sharing Project.

137 DOC concentrations were measured according to the method of Chen et al. (2021). Seawater were filtered through  
138 Whatman GF/F filters (precombusted at 500 °C for 4 h), and the filtrate was stored at -20 °C for DOC analyses. The  
139 DOC concentrations were determined by a total organic carbon analyzer (Shimadzu TOC-VCPH) after adding two  
140 drops of 12 mol/L HCl in the DOC samples.

## 141 **2.5 Data analysis**

142 To better understand the sources and sinks of the three VSCs and the factors affecting their distributions, SPSS 24.0  
143 software (SPSS Inc., Chicago, IL, USA) was used to analyze the relationships between environmental factors and the  
144 three VSCs in seawater and atmosphere during spring and summer.

## 145 **3 Results**

### 146 **3.1 Spatial distributions of COS, DMS, and CS<sub>2</sub> in surface seawater**

#### 147 **3.1.1 Spring distributions**

148 The temperature in the surface seawater showed a decreasing trend from south to north and the salinity increased from  
149 the inshore to offshore sites due to the influences of the Yellow Sea warm current, Yalu River, and Yellow River (Fig.  
150 2). The Chl *a* concentrations in the surface water of the BS and YS in the spring ranged between 0.17–4.45 μg L<sup>-1</sup>  
151 with an average of 1.19 ± 0.96 μg L<sup>-1</sup>. The highest Chl *a* concentration (4.45 μg L<sup>-1</sup>) occurred at station B39 in the  
152 Bohai (Fig. 2), which may be related to the enhanced phytoplankton growth from the abundance of nutrients due to  
153 the seawater exchange between the BS and YS. In addition, high Chl *a* concentrations were observed in the central  
154 area of the southern YS.

155 The concentrations of COS, DMS, and CS<sub>2</sub> in the surface seawater of the BS and YS during spring ranged between  
156 0.14–0.42, 0.41–7.74, and 0.01–0.18 nmol L<sup>-1</sup>, respectively, with mean values of 0.24 ± 0.06, 1.74 ± 1.61, and 0.07 ±



157 0.05 nmol L<sup>-1</sup> (Fig. 2). The high COS concentrations observed during the spring all occurred in the YS (Fig. 2). The  
158 highest COS concentration appeared at station H21 and coincided with a high Chl *a* concentration. At the same time,  
159 the two areas with high concentrations of COS in the central waters of the southern YS partially coincided with areas  
160 with high Chl *a* concentrations. High DMS concentrations existed in the coastal waters of the southern Shandong  
161 Peninsula as well as at station B21 in the central part of the northern YS. The distribution of CS<sub>2</sub> in seawater exhibited  
162 a decreasing trend from inshore to offshore (Fig. 2), which was similar with that of DOC. High CS<sub>2</sub> concentrations  
163 appeared at stations H18 and H19 in the coastal waters of YSCWM (Fig. 2). There was also a high CS<sub>2</sub> concentration  
164 at station B30 near the shore of the Liaodong Peninsula (Fig. 2).

### 165 3.1.2 Summer distributions

166 The temperature and salinity in the BS and YS in summer were relatively high and the high Chl *a* concentrations were  
167 concentrated in coastal waters (Fig. 3). The Chl *a* concentrations in the seawater during summer ranged between 0.10–  
168 4.74 μg L<sup>-1</sup> with an average of 1.60 ± 1.19 μg L<sup>-1</sup>. Station B43 near the Yellow River estuary had a high Chl *a*  
169 concentration (Fig. 3), which may have been due to the abundance of nutrients carried by nearby rivers or coastal  
170 currents. There were low salinities, high nitrate and Chl *a* concentrations at Stations H32, H34, and H35 in the  
171 northeast of Yangtze River Estuary, and Stations B66 and B68 near the Laizhou Bay and Yellow River Estuary (Fig.  
172 3 and S1).

173 The concentrations of COS, DMS, and CS<sub>2</sub> in the surface water of the BS and YS during summer were 0.32–0.61,  
174 1.31–18.12, and 0.01–0.65 nmol L<sup>-1</sup>, respectively, with mean values of 0.44 ± 0.06, 5.43 ± 3.60, and 0.26 ± 0.15 nmol  
175 L<sup>-1</sup> (Fig. 3). The mean concentrations of Chl *a*, COS, DMS, and CS<sub>2</sub> were 1.3-, 1.8-, 3.1-, and 3.7-fold higher in  
176 summer than spring. High COS concentrations were observed at stations B38 and B54 in the BS during summer. In  
177 addition, COS had a high concentration at station H25 in the central part of the southern YS, which was near where  
178 CS<sub>2</sub> also exhibited a high concentration (Fig. 3). High DMS concentrations were common in the northern BS, and  
179 were generally coincident with high Chl *a* levels. However, high Chl *a* and DMS concentrations were found in the  
180 coastal waters of the Yangtze River Estuary due to the Changjiang Diluted Water. In addition, the DMS concentration  
181 was high at station H12 (Fig. 3). There were high CS<sub>2</sub> concentrations in the northeastern area of the Yangtze River  
182 estuary (Fig. 3).



## 183 3.2 Depth distributions of COS, DMS, and CS<sub>2</sub> in seawater

### 184 3.2.1 Depth distributions in spring

185 There was a clear tendency for temperature and Chl *a* to gradually decreased from the surface to the bottom seawater  
186 (Fig. 4). The mean concentrations of Chl *a*, COS, DMS, and CS<sub>2</sub> were 5.4-, 5.1-, 5.9-, and 8.9-fold higher in the  
187 surface at about 4 m compared to > 60 m (Fig. 4). Consistent with the Chl *a* distribution, the depth distribution of  
188 DMS in the seawater decreased from the euphotic zone to the bottom seawater (Fig. 4). The high COS concentrations  
189 occurred in the surface seawater and decreased with depth, and the lowest concentrations occurred in the bottom  
190 waters. CS<sub>2</sub> exhibited obvious depth gradients at most stations during spring, with higher concentrations in the surface  
191 except for station H15, where the CS<sub>2</sub> concentrations were high in the bottom seawater.

### 192 3.2.2 Depth distributions in summer

193 In the 35°N section there was clear influence of the YSCWM in summer. There were obvious temperature differences  
194 between the surface seawater and bottom seawater in summer, and stratification in the water bodies was observed (Fig.  
195 5). A distinct thermocline emerged at a depth of 20 m, indicating that the YSCWM had formed (Fig. 5). The high Chl  
196 *a* concentrations in the surveyed area of the BS and YS during summer all occurred in the euphotic zone, and the  
197 highest concentrations occurred in the waters at depths of 10–20 m (Fig. 5). The mean Chl *a* concentrations were 5.4-  
198 fold higher at depths of 10–20 m compared to > 60 m. The depth distribution of DMS in seawater during summer  
199 decreased from the surface to the bottom seawater (Fig. 5). COS and CS<sub>2</sub> showed a significant depth gradient at most  
200 stations and decreased with the increasing depth. The mean concentrations of COS, DMS, and CS<sub>2</sub> were 17.5-, 21.6-,  
201 and 21.0-fold higher in the surface at about 3 m compared to > 60 m. However, in the bottom waters of station H16,  
202 COS had a relatively high concentration (Fig. 5). The mean concentrations of Chl *a*, COS, DMS, and CS<sub>2</sub> at different  
203 depths were 41.7-, 18.9-, 107-, and 37.6-fold higher in summer than spring.

## 204 3.3 VSCs in the atmosphere

### 205 3.3.1 Spring

206 The concentrations of COS, DMS, and CS<sub>2</sub> in the atmosphere overlying the BS and YS in spring were in the range of  
207 255.9–620.2 pptv, 1.3–191.2 pptv, and 5.2–698.8 pptv, respectively (Fig. 6a) and their mean concentrations were



208  $345.6 \pm 79.2$  pptv,  $47.5 \pm 49.8$  pptv, and  $113.2 \pm 172.3$  pptv. The decreasing order of the three VSCs mean  
209 concentrations in the atmosphere during spring was  $\text{COS} > \text{CS}_2 > \text{DMS}$ .

### 210 3.3.2 Summer

211 The concentrations of COS, DMS, and  $\text{CS}_2$  in summer ranged from 394.6 to 850.1 pptv, from 10.3 to 464.3 pptv, and  
212 from 15.3 to 672.7 pptv, respectively, with mean values of  $570.7 \pm 179.2$  pptv,  $223.8 \pm 143.6$  pptv, and  $180.3 \pm 235.6$   
213 pptv (Fig. 6b), and the order of the three VSCs in terms of mean concentrations in the atmosphere during summer was  
214  $\text{COS} > \text{DMS} > \text{CS}_2$ .

### 215 3.3.3 Seasonal variability of VSCs in the atmosphere

216 In spring, the highest concentration of atmospheric COS appeared at station B72 (Fig. 6a), which was located near the  
217 northern Shandong Peninsula. The highest atmospheric DMS concentration appeared at station B08 (Fig. 6a). At  
218 station B49, the DMS concentration in the seawater (Fig. 2) was not as high as that in the atmosphere (Fig. 6a).  
219 According to the 72 h backward trajectory map (Fig. S2), the air mass over station B49 had migrated from the land to  
220 the ocean, passing through Beijing, Tianjin, and other densely populated areas. The lowest atmospheric DMS  
221 concentration appeared at station B47 (Fig. 6a), probably due to the low DMS concentration in seawater ( $0.5 \text{ nmol L}^{-1}$ )  
222 <sup>1</sup>). In addition, there were high concentrations of  $\text{CS}_2$  at stations in the BS, such as B57, B60, and B72, and low  
223 concentrations at stations B17 and B21 in the northern YS (Fig. 6a).

224 The mean concentrations of atmospheric COS, DMS, and  $\text{CS}_2$  were 1.7-, 4.7-, and 1.6-fold higher in summer than  
225 spring. In summer, the three VSCs in the atmosphere over the BS and YS had similar spatial distributions. At station  
226 B64, both COS and DMS exhibited their highest concentrations (Fig. 6b). The highest concentration of  $\text{CS}_2$  in summer  
227 appeared at station B49 near the shore, and the lowest concentration appeared far from shore at station H09 (Fig. 6b).  
228 The distributions of  $\text{CS}_2$  showed an obvious decreasing trend from inshore to offshore (Fig. 6b).

### 229 3.4 Relationships among COS, DMS, and $\text{CS}_2$ and environment factors

230 A positive correlation was found between COS and DOC in seawater during summer ( $P > 0.05$ ) (Table S4). There  
231 was no significant correlation among the three VSCs in seawater in spring ( $P > 0.05$ ), but there was a significant  
232 correlation between COS and  $\text{CS}_2$  in the atmosphere ( $P < 0.01$ ) (Table S3). A significant correlation was found



233 between DMS and CS<sub>2</sub> in surface seawater in summer ( $P < 0.01$ , Table S4). In addition, there was a significant  
234 correlation between atmospheric COS and CS<sub>2</sub> in summer ( $P < 0.01$ , Table S4). The correlations between the three  
235 oceanic VSCs and atmospheric VSCs were not significant ( $P > 0.05$ , Table S3 and S4).

### 236 3.5 Sea-to-air fluxes of VSCs

#### 237 3.5.1 Spring

238 The sea-to-air fluxes of COS, DMS, and CS<sub>2</sub> in spring were 0.01–1.59, 0.06–25.40, and 0.002–0.42  $\mu\text{mol m}^{-2} \text{d}^{-1}$ ,  
239 respectively, with averages of  $0.46 \pm 0.35$ ,  $2.99 \pm 4.24$ , and  $0.10 \pm 0.10 \mu\text{mol m}^{-2} \text{d}^{-1}$  (Fig. 7). The highest COS sea-  
240 to-air flux appeared at station B36, which had a high wind speed ( $11.3 \text{ m s}^{-1}$ ). In comparison, the lowest COS sea-  
241 air flux occurred at station H01, where the minimum wind speed occurred ( $0.4 \text{ m s}^{-1}$ ); the lowest sea-to-air fluxes of  
242 DMS and CS<sub>2</sub> also occurred at station H01 (Fig. 7). The highest DMS and CS<sub>2</sub> sea-to-air fluxes appeared at stations  
243 HS4 and B70, respectively, due to high wind speeds and DMS and CS<sub>2</sub> concentrations (Fig. 7).

#### 244 3.5.2 Summer

245 The sea-to-air fluxes of COS, DMS, and CS<sub>2</sub> in summer were 0.02–2.47, 0.10–25.44, and 0.003–1.72  $\mu\text{mol m}^{-2} \text{d}^{-1}$ ,  
246 respectively, with the averages of  $0.59 \pm 0.52$ ,  $6.26 \pm 6.27$ , and  $0.30 \pm 0.32 \mu\text{mol m}^{-2} \text{d}^{-1}$  (Fig. 8). The mean sea-to-air  
247 fluxes of COS, DMS, and CS<sub>2</sub> were 1.3-, 2.1-, and 3.0-fold higher in summer than spring. Consistent with their order  
248 in seawater, the order of the sea-to-air fluxes of the VSCs was DMS > COS > CS<sub>2</sub>. The lowest sea-to-air fluxes of  
249 VSCs in summer occurred at station B05, which had the lowest wind speed ( $0.4 \text{ m s}^{-1}$ ) and low seawater concentrations  
250 of VSCs. The highest sea-to-air flux of COS and DMS appeared at stations B23 and H14, respectively, coinciding  
251 with high wind speeds and high COS and DMS concentrations in seawater (Fig. 8). The maximum CS<sub>2</sub> sea-to-air flux  
252 appeared at station H28, where the concentration of CS<sub>2</sub> in seawater was high (Fig. 8).

## 253 4 Discussion

### 254 4.1 Spatial and depth distributions of three VSCs in seawater

#### 255 4.1.1 Spatial distributions



256 The COS concentrations in this study were similar to those in six tidal European estuaries (Scheldt, Gironde, Rhine,  
257 Elbe, Ems, and Loire) ( $0.22 \text{ nmol L}^{-1}$ ) (Sciare et al., 2002), the DMS concentrations were lower than previous  
258 observations in the BS and YS in autumn ( $3.92 \text{ nmol L}^{-1}$ ) (Yang et al., 2014), and the  $\text{CS}_2$  concentrations were lower  
259 than those in the coastal waters off the eastern coast of the United States ( $0.004\text{--}0.51 \text{ nmol L}^{-1}$ ) (Kim and Andreae,  
260 1992). Besides, the VSC concentrations in the seawater of the BS and YS were significantly higher than those in the  
261 oceanic areas such as the North Atlantic Ocean (Simó et al., 1997; Ulshöfer et al., 1995). Zepp and Andreae (1994)  
262 also showed that COS concentrations in nearshore waters were 40-fold higher than those in the open sea waters. The  
263 higher CDOM concentrations in the nearshore waters may be the reason of the difference (Gueguen et al., 2005).

264 Different production and consumption mechanisms led to the spatial distributions of COS, DMS, and  $\text{CS}_2$  being  
265 different. DMS and DMSP concentrations are related to the composition and abundance of phytoplankton (Kurian et  
266 al., 2020; Naik et al., 2020; O'Brien et al., 2022). The highest DMS concentrations at station B21 in spring coincided  
267 with high Chl *a* concentrations (Fig. 2). Low salinities ( $< 30$ ) appeared at stations of H25, H26, H34, H35, B43, B66,  
268 and B68 due to river water discharge from Yangtze River Estuary, Yellow River and Laizhou Bay were consistent  
269 with high nitrate, Chl *a*, and DMS concentrations (Fig. 3 and S1). High  $\text{CS}_2$  concentrations in the coastal waters of  
270 the Yellow River estuary and at stations H18, H19, B30 in spring may be due to high CDOM carried by the Yellow  
271 Sea coastal current and Yellow River and terrestrial input. The emergence of high- $\text{CS}_2$ -value areas in the YS may  
272 have been because the Yangtze River experiences a flood season during summer and large amounts of sediment are  
273 carried into the sea, making the coastal waters of the South Yellow Sea (especially the surface seawater) more turbid,  
274 while the open seas were affected less by the Yangtze River and were more transparent. With higher transparency,  
275 light-induced reactions in water are more likely to occur. The significant correlation between DMS and  $\text{CS}_2$  in surface  
276 seawater in summer was consistent with the results of Ferek and Andreae (1983) and Yu et al. (2022). DMS in seawater  
277 is mainly derived from the degradation of DMSP, which is released from algal cell lysis (O'Brien et al., 2022).  
278 Moreover, the algae decay increased  $\text{CS}_2$  emission rate for the reason of degradation of sulfur-containing amino acids  
279 (Wang et al., 2023). The commonality of their sources resulted in a good correlation between DMS and  $\text{CS}_2$  in seawater.  
280 Xie et al. (1998) pointed out that  $\text{CS}_2$  has a photochemical production mechanism that is similar to that of COS, and  
281 both are primarily produced by photochemical reactions of thiol-containing compounds such as methyl mercaptan  
282 (MeSH) or glutathione under the catalysis of CDOM. Terrestrial CDOM had higher photochemical reactivity and was  
283 more conducive to the photochemical generation of  $\text{CS}_2$  (Xie et al., 1998). COS and  $\text{CS}_2$  are formed via reaction



284 between cysteine and intermediates (e.g., CDOM,  $\cdot\text{OH}$ ) (Chu et al., 2016; Du et al., 2017; Modiri Gharehveran et al.,  
285 2020). Modiri Gharehveran and Shah (2021) proposed that DOM can photochemically produce  $^3\text{CDOM}^*$ ,  $^1\text{O}_2$ ,  $\text{H}_2\text{O}_2$ ,  
286 and  $\cdot\text{OH}$  via sunlight, which react with DMS and form a sulfur- or - carbon centered radical and then COS and  $\text{CS}_2$ .  
287 High COS concentrations in spring may be due to the influence of the sediment input from the Yellow River into the  
288 BS, which was more turbid and not conducive to the photochemical production of COS. Li et al. (2022) demonstrated  
289 that high nitrate concentration played a key role in high COS production. Two high COS concentrations at stations  
290 H25 and B43 during summer coincided with high nitrate concentration. However, no significant correlations were  
291 found between COS and nitrate concentrations for all the stations during both spring and summer (Tables S3 and S4).  
292 Zepp and Andreae (1994) showed that the photochemical production rates of COS were higher in coastal waters than  
293 in the open sea. Flück et al. (1997) also believed that the photochemical production of COS benefited from the catalysis  
294 by CDOM. Uher and Andreae (1997) showed that COS in seawater was significantly correlated with CDOM,  
295 indicating that organic compounds affect the concentrations and distributions of COS in seawater. The positive  
296 correlation between COS and DOC in seawater during summer was consistent with Uher and Andreae (1997).

297 The VSCs in seawater exhibited significant seasonal differences between spring and summer in this study. Xu et al.  
298 (2001) observed that the COS concentrations in the R/V *Polarstern* of South Africa in summer were higher than those  
299 in autumn. In addition, observations by Weiss et al. (1995) showed that the COS concentrations in the seawater of the  
300 Atlantic and Pacific Oceans were very low in winter. In this study, the concentrations of the three VSCs in seawater  
301 during summer were higher than those in spring, which may be due to the higher Chl *a* in summer (mean:  $1.60 \mu\text{g L}^{-1}$ )  
302 than in spring (mean:  $1.19 \mu\text{g L}^{-1}$ ). Similar to the seasonal changes in Chl *a*, DMS concentrations were higher in  
303 summer than in spring. Indeed, higher phytoplankton biomass in summer has been linked to higher DMS  
304 concentrations in summer than in autumn (Yang et al., 2015). Our results showed that the average concentrations of  
305 COS, DMS, and  $\text{CS}_2$  in the surface seawater of the BS and YS during summer were higher than those during spring,  
306 and also higher than those in the Changjiang estuary and the adjacent East China Sea (Yu et al., 2022). Different sea  
307 areas, temperature, and industry production may be the difference reasons, and in terms of the latter, the rayon  
308 production which is the main source of anthropogenic  $\text{CS}_2$  (Campbell et al., 2015) in the northern city of BS.

#### 309 **4.1.2 Depth distributions**

310 DMS, COS and  $\text{CS}_2$  showed similar patterns and decreased with the increasing depth, which agreed with the results  
311 in Yu et al (2022). The highest Chl *a* concentrations during summer occurred at depths of 10–20 m. This was mainly



312 due to the abundance of nutrients and suitable water temperature near the thermocline, which benefitted phytoplankton  
313 growth. DMS is mainly originated from phytoplankton and coincided with Chl *a* changing pattern. COS and CS<sub>2</sub> in  
314 seawater were mainly derived from photochemical reactions of organic sulfides catalyzed by CDOM, so light became  
315 the limiting factor for their production in seawater (Uher and Andreae, 1997). Ulshöfer et al. (1996) studied the depth  
316 distribution of COS in seawater and found that the high concentrations of COS all appeared in the euphotic zone. High  
317 COS concentrations in the surface seawater in spring in this study may be due to the fact that the photochemical  
318 production reactions of CS<sub>2</sub> and COS mainly occurred in the euphotic zone because they are dependent on light (Flöck  
319 et al., 1997; Xie et al., 1998). Hobe et al. (2001) argued that non-photochemical production of COS plays an important  
320 role in its global budget. Consistent with Hobe et al. (2001), high COS concentration in the bottom waters of station  
321 H16 in summer may be related to the non-photochemical production of COS or release by underlying sediments. High  
322 CS<sub>2</sub> concentrations in the bottom seawater at station H15 in spring may be caused by release from the underlying  
323 sediments. Jørgensen and Okholm-Hansen (1985) found that the release rate of VSCs (such as CS<sub>2</sub>) in oxygen-  
324 containing surface seawater was usually 10 to 100 times lower than that in underlying sediments in a Danish estuary,  
325 indicating that release from sediments is an important source of CS<sub>2</sub>. It has been shown that CS<sub>2</sub> can be produced by  
326 anaerobic fermentation by bacteria and by reactions between H<sub>2</sub>S and organic matter in pore water (and anoxic basins)  
327 (Andreae, 1986). This hypothesis agreed with the results of Wakeham et al. (1987), where the concentration of CS<sub>2</sub>  
328 peaked (at about 20 nmol L<sup>-1</sup>) near the sediment-water interface.

#### 329 **4.2 VSCs in the atmosphere**

330 Similar to our results for VSCs concentrations in the atmosphere during summer, Kettle et al. (2001) found that the  
331 COS concentration in the Atlantic Ocean atmosphere was 552 pptv and Cooper and Saltzman (1993) measured a DMS  
332 concentration of 118 pptv. In addition, the concentrations of atmospheric CS<sub>2</sub> in this study were similar to  
333 concentrations of CS<sub>2</sub> observed in a polluted atmosphere (Sandalls and Penkett, 1977), but much higher than the CS<sub>2</sub>  
334 concentration in unpolluted atmospheres such as over the North Atlantic (Cooper and Saltzman, 1993). This indicated  
335 that industrial production and human activities had a significant impact on the concentration of CS<sub>2</sub> in the atmosphere.  
336 The mean VSCs concentrations in the atmosphere during summer in this study were all higher than those in the  
337 Changjiang estuary and the adjacent East China Sea (Yu et al., 2022) due to different areas.



338 The difference in the order of atmospheric VSC concentrations between spring and summer was mainly due to the  
339 high DMS concentrations in the surface seawater during summer. The concentrations of VSCs in the atmosphere  
340 during summer were much higher than in spring, which may be attributed to anthropogenic activities and industrial  
341 emissions. Chin and Davis (1993) showed that anthropogenic sources can significantly affect the concentration of  
342 VSCs in the atmosphere. Anthropogenic VSCs emissions can be evaluated by using isotope measurements (Hattori et  
343 al., 2020). Unfortunately, anthropogenic VSCs emissions were not evaluated in this study, and isotope measurements  
344 will be further studied in the future. In addition, the seasonal changes in the COS, DMS, and CS<sub>2</sub> concentrations in  
345 the atmosphere overlying the BS and YS were consistent with those in seawater. Therefore, the high concentrations  
346 of atmospheric COS, DMS, and CS<sub>2</sub> during summer were likely associated with high VSCs concentrations in seawater,  
347 which meant that sea-to-air diffusion was an important source of atmospheric VSCs. However, no significance was  
348 found between VSCs in the seawater and atmosphere, which may be because that VSCs in the atmosphere were not  
349 only from sea-to-air diffusion, but also from complex sources such as soil, incomplete burning of biomass, and  
350 industrial releases (Chin and Davis, 1993).

351 The distributions of atmospheric COS above the BS and YS were relatively consistent with respect to their  
352 concentrations in seawater, which was related to the chemical inertness of COS in the atmosphere (Crutzen, 1976). In  
353 spring, the highest concentration of atmospheric COS at station B72 and DMS at station B08 may coincided with the  
354 anthropogenic emissions and high DMS concentration in seawater, respectively (Fig. 6). The CS<sub>2</sub> generated by  
355 industrial activities may influence the atmosphere at station B49 which is near industrial cities like Tianjin. Studies  
356 have shown that anthropogenic input accounts for about 50% of the total CS<sub>2</sub> in the global atmosphere, and both  
357 chemical production and pharmaceutical industries are large emitters of CS<sub>2</sub> into the atmosphere (Chin and Davis,  
358 1993). CS<sub>2</sub> is the main precursor of COS in the atmosphere, and atmospheric CS<sub>2</sub> is oxidized to COS by radicals such  
359 as OH with a conversion efficiency of 0.81 (Chin and Davis, 1995). Significant correlation between atmospheric COS  
360 and CS<sub>2</sub> in our study demonstrated this.

361 The 72 h backward trajectory map over station B49 indicated that the high atmospheric DMS concentration was  
362 produced by human activities. The highest concentrations of COS and DMS at station B64 in summer may be caused



363 by anthropogenic emissions in the coastal region. The highest CS<sub>2</sub> concentration in summer at station B49 near  
364 industrial cities like Tianjin may be related to the CS<sub>2</sub> generation by industrial activities.

#### 365 **4.3 Sea-to-air fluxes of VSCs**

366 The spatial variability in sea-to-air fluxes were consistent with changes in wind speed, which was because sea-to-air  
367 fluxes are dependent on the transmission velocities of VSCs in seawater, which are related to wind speed and viscosity  
368 of seawater, i.e., the highest COS sea-to-air flux at station B36 and the lowest three VSCs sea-to-air flux at station  
369 H01 in spring (Fig. 7). Besides wind speed, the oceanic VSCs concentrations are related to the sea-to-air fluxes, i.e.,  
370 highest DMS and CS<sub>2</sub> sea-to-air fluxes at stations HS4 and B70 in spring (Fig. 7). Wind speed was the main influencing  
371 factor compared with the concentration of VSCs in the seawater. Although the oceanic VSCs concentrations at station  
372 H01 were high, the low wind speed reduced the transmission velocity of the VSCs at the sea-to-air interface in this  
373 region, resulting in low sea-to-air fluxes.

374 In addition, the sea-to-air fluxes of all three VSCs in both spring and summer were positive, indicating that the  
375 seawater was a source of COS, DMS, and CS<sub>2</sub> to the atmosphere through sea-to-air diffusion. However, while our  
376 findings agreed with Chin and Davis (1993) and Yu et al. (2022) who showed that the ocean was a major atmospheric  
377 source of COS, they conflicted with Weiss et al. (1995) and Zhu et al. (2019) who found significant COS  
378 undersaturation in some seas. Therefore, the ocean may become a sink of atmospheric COS in some areas or times of  
379 year. The results of this study, which covered offshore and inshore areas, showed that most of coastal and estuarine  
380 seas were sources of COS in the atmosphere, but open seas can have markedly lower concentrations of COS and may  
381 become sinks of COS from the atmosphere under the right conditions. The ocean was the main atmospheric source of  
382 DMS and CS<sub>2</sub> due to their low concentrations in atmosphere.

#### 383 **5 Conclusions**

384 The distributions of COS, DMS, and CS<sub>2</sub> in the surface seawater and marine atmosphere of the BS and YS during  
385 spring and summer exhibited significant spatial and seasonal variability. First, COS, DMS, and CS<sub>2</sub> had higher  
386 concentrations in summer than in spring. Second, both COS and CS<sub>2</sub> had higher concentrations in coastal waters than  
387 in offshore waters, which may due to higher photochemical reaction rates in nearshore waters compared with the open  
388 sea. In summer, areas with similarly high values of COS and CS<sub>2</sub> emerged, indicating that they may have common



389 photochemical production mechanisms. The depth distributions of COS, DMS, and CS<sub>2</sub> were characterized by high  
390 concentrations in the surface seawater that decreased with depth.

391 In addition, the atmospheric VSC concentrations of the BS and YS exhibited obvious seasonal differences, with  
392 higher concentrations in the summer than in the spring. The VSCs in the atmosphere over the BS and YS had similar  
393 spatial distributions, with declining trends from inshore to offshore areas, especially for CS<sub>2</sub>. This phenomenon  
394 illustrated the effect of anthropogenic emissions on the atmospheric concentrations of VSCs. Finally, high sea-to-air  
395 fluxes of COS, DMS, and CS<sub>2</sub> in the BS and YS indicated that marginal seas were major sources of atmospheric VSCs  
396 and may make considerable contributions to the global sulfur budget.

397 *Data availability.* Data to support this article are available at <https://doi.org/10.6084/m9.figshare.14971644>.

398 *Author contributions.* All authors were involved in the writing of the paper and approved the final submitted paper.

399 YJ and YL were major contributors to the study's conception, data analysis and drafting of the paper. HZ, LJG and  
400 LQ contributed significantly to writing-original draft. YGP contributed to writing-reviewing, and editing.

401 *Competing interests.* The authors declare that they have no conflict of interest.

402 *Acknowledgements.* We are grateful to the captain and crew of the R/V “*Dong Fang Hong 2*” for their help and  
403 cooperation during the in situ investigation.

404 *Financial support.* This work was funded by the National Natural Science Foundation of China (41976038, 41876122),  
405 and the National Key Research and Development Program (2016YFA0601301).

## 406 **References**

407 Andreae, M. O.: The ocean as a source of atmospheric sulfur compounds, in: The role of air-sea exchange in  
408 geochemical cycling, edited by: Buat-Ménard, P., Springer, Berlin, Heidelberg, Germany, 331–362,  
409 [https://doi.org/10.1007/978-94-009-4738-2\\_9](https://doi.org/10.1007/978-94-009-4738-2_9), 1986.

410 Andreae, M. O., and Crutzen, P. J.: Atmospheric aerosols: biogeochemical sources and role in atmospheric chemistry,  
411 *Science*, 276 (5315), 1052–1058, <https://doi.org/10.1126/science.276.5315.1052>, 1997.

412 Aydin, M., Britten, G. L., Montzka, S. A., Buizert, C., Primeau, F. W., Petrenko, V. V., Battle, M. O., Nicewonger,  
413 M. R., Patterson, J., Hmiel, B., and Saltzman, E. S.: Anthropogenic impacts on atmospheric carbonyl sulfide since  
414 the 19th century inferred from polar firn air and ice core measurements, *J. Geophys. Res.-Atmos.*, 125(16),



- 415 e2020JD033074, <https://doi.org/10.1002/essoar.10503126.1>, 2020.
- 416 Brown, A. S., van der Veen, A. M. H., Arrhenius, K., Murugan, A., Culleton, L. P., Ziel, P. R., and Li, J.: Sampling  
417 of gaseous sulfur-containing compounds at low concentrations with a review of best-practice methods for biogas  
418 and natural gas applications, *Trac-Trends Anal. Chem.*, 64, 42–52, <https://doi.org/10.1016/j.trac.2014.08.012>, 2015.
- 419 Brihl, C., Lelieveld, J., Crutzen, P. J., and Tost, H.: The role of carbonyl sulphide as a source of stratospheric sulphate  
420 aerosol and its impact on climate, *Atmos. Chem. Phys.*, 12(3), 1239–1253, [http://dx.doi.org/10.5194/acp-12-1239-](http://dx.doi.org/10.5194/acp-12-1239-2012)  
421 2012, 2012.
- 422 Campbell, J. E., Carmichael, G. R., Chai T., Mena-Carrasco, M., Tang, Y., Blake, D. R., Blake, N. J., Vay, S. A.,  
423 Collatz, G. J., Baker, I., Berry, J. A., Montzka, S. A., Sweeney, C., Schnoor, J. L., and Stanier, C. O.: Photosynthetic  
424 control of atmospheric carbonyl sulfide during the growing season, *Science*, 322, 1085–1088,  
425 <https://doi.org/10.1126/science.1164015>, 2008.
- 426 Campbell, J. E., Whelan, M. E., Seibt U., Smith S. J., Berry, J. A., and Hilton, T. W.: Atmospheric carbonyl sulfide  
427 sources from anthropogenic activity: Implications for carbon cycle constraints, *Geophys. Res. Lett.*, 42, 3004–3010,  
428 <https://doi.org/10.1002/2015GL063445>, 2015.
- 429 Charlson, R. J., Lovelock, J. E., Andreae, M. O., and Warren, S. G.: Oceanic phytoplankton, atmospheric sulphur,  
430 cloud albedo and climate, *Nature*, 326, 655–661, <https://doi.org/10.1038/326655a0>, 1987.
- 431 Chen C.-T. A.: Chemical and physical fronts in the Bohai, Yellow and East China seas, *J. Mar. Syst.*, 78(3), 394–410,  
432 <https://doi.org/10.1016/j.jmarsys.2008.11.016>, 2009.
- 433 Chen, Y., Wang, P., Shi, D., Ji, C.-X., Chen, R., Gao, X.-C., and Yang, G.-P.: Distribution and bioavailability of  
434 dissolved and particulate organic matter in different water masses of the Southern Yellow Sea and East China Sea,  
435 *J. Marine Syst.*, 222, 103596, <https://doi.org/10.1016/j.jmarsys.2021.103596>, 2021.
- 436 Chin, M., and Davis, D. D.: Global sources and sinks of OCS and CS<sub>2</sub> and their distributions, *Global Biogeochem.*  
437 *Cy.*, 7(2), 321–337, <https://doi.org/10.1029/93GB00568>, 1993.
- 438 Chin, M., and Davis, D. D.: A reanalysis of carbonyl sulfide as a source of stratospheric background sulfur aerosol, *J.*  
439 *Geophys. Res.-Atmos.*, 100(D5), 8993–9005, <https://doi.org/10.1029/95JD00275>, 1995.



- 440 Chu, C., Erickson, P. R., Lundeen, R. A., Stamatelatos, D., Alaimo, P. J., Latch D. E., and McNeill, K.: Photochemical  
441 and nonphotochemical transformations of cysteine with dissolved organic matter, *Environ. Sci. Technol.*, 50, 6363–  
442 6373, <https://doi.org/10.1021/acs.est.6b01291>, 2016.
- 443 Cline, J. D., and Bates, T. S.: Dimethyl sulfide in the Equatorial Pacific Ocean: a natural source of sulfur to the  
444 atmosphere, *Geophys. Res. Lett.*, 10(10), 949–952, <https://doi.org/10.1029/GL010i010p00949>, 1983.
- 445 Cooper, D. J., and Saltzman, E. S.: Measurements of atmospheric dimethylsulfide, hydrogen sulfide, and carbon  
446 disulfide during GTE/CITE 3, *J. Geophys. Res.-Atmos.*, 98(D12), 23397–23409,  
447 <https://doi.org/10.1029/92JD00218>, 1993.
- 448 Crutzen, P. J.: The possible importance of CSO for the sulfate layer of the stratosphere, *Geophys. Res. Lett.*, 3(2), 73–  
449 76, <https://doi.org/10.1029/GL003i002p00073>, 1976.
- 450 Curson, A. R. J., Liu, J., Bermejo Martínez, A., Green, R. T., Chan, Y., Carrión, O., Williams, B. T., Zhang, S.-H.,  
451 Yang, G.-P., Bulman Page, P. C., Zhang, X.-H., and Todd, J. D.: Dimethylsulfoniopropionate biosynthesis in marine  
452 bacteria and identification of the key gene in this process, *Nat. Microbiol.*, 2: 17009,  
453 <https://doi.org/10.1038/nmicrobiol.2017.9>, 2017.
- 454 Du, Q., Mu, Y., Zhang, C., Liu, J., Zhang, Y., and Liu, C.: Photochemical production of carbonyl sulfide, carbon  
455 disulfide and dimethyl sulfide in a lake water, *J. Environ. Sci.*, 51, 146–156,  
456 <https://doi.org/10.1016/j.jes.2016.08.006>, 2017.
- 457 Ferek, R. J., and Andreae, M. O.: The supersaturation of carbonyl sulfide in surface waters of the Pacific Ocean off  
458 Peru, *Geophys. Res. Lett.*, 10(5), 393–396, <https://doi.org/10.1029/GL010I005P00393>, 1983.
- 459 Flück, O. R., Andreae, M. O., and Dräger, M.: Environmentally relevant precursors of carbonyl sulfide in aquatic  
460 systems, *Mar. Chem.*, 59(1-2), 71–85, [https://doi.org/10.1016/S0304-4203\(97\)00012-1](https://doi.org/10.1016/S0304-4203(97)00012-1), 1997.
- 461 Guéguen, C., Guo, L., and Tanaka, N.: Distributions and characteristics of colored dissolved organic matter in the  
462 Western Arctic Ocean, *Cont. Shelf Res.*, 25, 1195–1207, <https://doi.org/10.1016/j.csr.2005.01.005>, 2005.
- 463 Hattori, S., Kamezaki, K., and Yoshida, N.: Constraining the atmospheric OCS budget from sulfur isotopes, *Proc.*  
464 *Natl. Acad. Sci. U.S.A.*, 117(34), 20447–20452, <https://doi.org/10.1073/pnas.2007260117>, 2020.
- 465 Hobe, M. V., Cutter, G. A., Kettle, A. J., and Andreae, M. O.: Dark production: a significant source of oceanic COS,



- 466 J. Geophys. Res.-Oceans., 106(C12), 31217–31226, <https://doi.org/10.1029/2000JC000567>, 2001.
- 467 Inomata, Y., Hayashi, M., Osada, K., and Iwasaka, Y.: Spatial distributions of volatile sulfur compounds in surface  
468 seawater and overlying atmosphere in the northwestern Pacific Ocean, eastern Indian Ocean, and Southern Ocean,  
469 Global Biogeochem. Cy., 20(2), GB2022, <https://doi.org/10.1029/2005GB002518>, 2006.
- 470 Jørgensen, B. B., and Okholm-Hansen, B.: Emissions of biogenic sulfur gases from a Danish estuary, Atmos. Environ.,  
471 19, 1737–1749, [https://doi.org/10.1016/0004-6981\(85\)90001-0](https://doi.org/10.1016/0004-6981(85)90001-0), 1985.
- 472 Keller, M. D., Bellows, W. K., and Guillard, R. R. L.: Dimethyl sulfide production in marine phytoplankton, in:  
473 Biogenic sulfur in the environment, edited by: Millero, F. J., Hershey, J. P., Saltzman, E. S., and Cooper, W. J.,  
474 American Chemical Society, Washington, DC, 167–182, <http://dx.doi.org/10.1021/bk-1989-0393.ch011>, 1989.
- 475 Kettle, A. J., Kuhn, U., von Hobe, M., Kesselmeier, J., and Andreae, M. O.: Global budget of atmospheric carbonyl  
476 sulfide: temporal and spatial variations of the dominant sources and sinks, J. Geophys. Res., 107(D22), 4658,  
477 <https://doi.org/10.1029/2002JD002187>, 2002.
- 478 Kettle, A. J., Rhee, T. S., von Hobe, M., Poulton, A., Aiken, J., and Andreae, M. O.: Assessing the flux of different  
479 volatile sulfur gases from the ocean to the atmosphere, J. Geophys. Res.-Atmos., 106(D11), 12193–12209,  
480 <https://doi.org/10.1029/2000JD900630>, 2001.
- 481 Kim, K.-H., and Andreae, M. O.: Carbon disulfide in estuarine, coastal and oceanic environments, Mar. Chem., 40,  
482 179–197, [https://doi.org/10.1016/0304-4203\(92\)90022-3](https://doi.org/10.1016/0304-4203(92)90022-3), 1992.
- 483 Kurian S, Chndrasekhararao A. V., Vidya P. J., Shenoy D. M., Gauns M., Uskaikar, H., and Aparna, S. G.: Role of  
484 oceanic fronts in enhancing phytoplankton biomass in the eastern Arabian Sea during an oligotrophic period, Mar.  
485 Environ. Res., 160, 105023, <https://doi.org/10.1016/j.marenvres.2020.105023>, 2020.
- 486 Lennartz, S. T., Marandino, C. A., von Hobe, M., Andreae, M. O., Aranami, K., Atlas, E., Berkelhammer, M.,  
487 Bingemer, H., Booge, D., Cutter, G., Cortes, P., Kremser, S., Law, C. S., Marriner, A., Simó R., Quack, B., Uher,  
488 G., Xie, H., and Xu, X.: Marine carbonyl sulfide (OCS) and carbon disulfide (CS<sub>2</sub>): a compilation of measurements  
489 in seawater and the marine boundary layer, Earth Syst. Sci. Data, 12, 591–609, <https://doi.org/10.5194/essd-12-591-2020>,  
490 591–2020, 2020.
- 491 Lennartz, S. T., Marandino, C. A., von Hobe, M., Cortes, P., Quack, B., Simo, R., Booge, D., Pozzer, A., Steinhoff,



- 492 T., Arevalo-Martinez, D. L., Kloss, C., Bracher, A., Röttgers, R., Atlas, E., and Krüger, K.: Direct oceanic emissions  
493 unlikely to account for the missing source of atmospheric carbonyl sulfide, *Atmos. Chem. Phys.*, 17, 385–402,  
494 <https://doi.org/10.5194/acp-17-385-2017>, 2017.
- 495 Li, J.-L., Zhai, X., and Du, L.: Effect of nitrate on the photochemical production of carbonyl sulfide from surface  
496 seawater, *Geophys. Res. Lett.*, 49, e2021GL097051, <https://doi.org/10.1029/2021GL097051>, 2022.
- 497 Liss, P. S., and Slater, P. G.: Flux of gases across the air-sea interface, *Nature*, 247(5438), 181–184,  
498 <https://doi.org/10.1038/247181a0>, 1974.
- 499 Maignan, F., Abadie, C., Remaud, M., Kooijmans, L. M. J., Kohonen, K.-M., Commane, R., Wehr, R., Campbell, J.  
500 E., Belviso, S., Montzka, S. A., Raoult, N., Seibt, U., Shiga, Y. P., Vuichard, N., Whelan, M. E., and Peylin, P.:  
501 Carbonyl sulfide: comparing a mechanistic representation of the vegetation uptake in a land surface model and the  
502 leaf relative uptake approach, *Biogeosciences*, 18, 2917–2955, <https://doi.org/10.5194/bg-18-2917-2021>, 2021.
- 503 Modiri Gharehveran, M., Hain E, Blaney L, and Shah, A. D.: Influence of dissolved organic matter on carbonyl sulfide  
504 and carbon disulfide formation from cysteine during sunlight photolysis, *Environ. Sci.: Processes Impacts*, 22,  
505 1852–1864, <https://doi.org/10.1039/DOEM00219D>, 2020.
- 506 Modiri Gharehveran, M., and Shah, A. D.: Influence of dissolved organic matter on carbonyl sulfide and carbon  
507 disulfide formation from dimethyl sulfide during sunlight photolysis, *Water Environ. Res.*, 93, 2982–2997,  
508 <https://doi.org/10.1002/wer.1650>, 2021.
- 509 Naik, B. R., Gauns, M., Bepari, K., Uskaikar, H., and Shenoy, D. M.: Variation in phytoplankton community and its  
510 implication to dimethylsulphide production at a coastal station off Goa, India, *Mar. Environ. Res.*, 157, 104926,  
511 <https://doi.org/10.1016/j.marenvres.2020.104926>, 2020.
- 512 Nightingale, P. D., Malin, G., Law, C. S., Watson, A. J., Liss, P. S., Liddicoat, M. I., Boutin, J., and Upstill-Goddard,  
513 R. C.: In situ evaluation of air-sea gas exchange parameterizations using novel conservative and volatile tracers,  
514 *Global Biogeochem. Cy.*, 14(1), 373–387, <https://doi.org/10.1029/1999GB900091>, 2000.
- 515 O'Brien, J., McParland, E. L., Bramucci, A. R., Ostrowski, M., Siboni, N., Ingleton, T., Brown, M. V., Levine, N. M.,  
516 Laverock, B., Petrou, K., and Seymour, J.: The microbiological drivers of temporally dynamic  
517 dimethylsulfoniopropionate cycling processes in Australian coastal shelf waters, *Front. Microbiol.*, 13, 894026,  
518 <https://doi.org/10.3389/fmicb.2022.894026>, 2022.



- 519 Parsons, T. R., Maita, Y., and Lalli, C. M.: A manual of chemical and biological methods for seawater analysis, in  
520 Fluorometric determination of chlorophylls, edited by: Parsons, T. R., Maita, Y., and Lalli, C. M., Great Britain,  
521 CA: Pergamon Press, 107–109, 1984.
- 522 Remaud, M., Chevallier, F., Maignan, F., Belviso, S., Berchet, A., Parouffe, A., Abadie, C., Bacour, C., Lennartz, S.,  
523 and Peylin, P.: Plant gross primary production, plant respiration and carbonyl sulfide emissions over the globe  
524 inferred by atmospheric inverse modelling, *Atmos. Chem. Phys.*, 22(4), 2525–2552, [https://doi.org/10.5194/acp-](https://doi.org/10.5194/acp-22-2525-2022)  
525 [22-2525-2022](https://doi.org/10.5194/acp-22-2525-2022), 2022.
- 526 Sandalls, F. J., and Penkett, S. A.: Measurements of carbonyl sulphide and carbon disulphide in the atmosphere, *Atmos.*  
527 *Environ.*, 11(2), 197–199, [https://doi.org/10.1016/0004-6981\(77\)90227-X](https://doi.org/10.1016/0004-6981(77)90227-X), 1977.
- 528 Sander, R.: Compilation of Henry's law constants (version 4.0) for water as solvent, *Atmos. Chem. Phys.*, 15, 4399–  
529 4981, <https://doi.org/10.5194/acp-15-4399-2015>, 2015.
- 530 Schäfer, H., Myronova, N., and Boden, R.: Microbial degradation of dimethylsulphide and related C<sub>1</sub>-sulphur  
531 compounds: organisms and pathways controlling fluxes of sulphur in the biosphere, *J. Exp. Bot.*, 61(2), 315–334,  
532 <https://doi.org/10.1093/jxb/erp355>, 2010.
- 533 Schlitzer, R.: Ocean Data View, [odv.awi.de](http://odv.awi.de), 2023.
- 534 Sciare, J., Mihalopoulos, N., and Nguyen, B. C.: Spatial and temporal variability of dissolved sulfur compounds in  
535 European estuaries, *Biogeochemistry*, 59(1–2), 121–141, <http://dx.doi.org/10.1023/A:1015539725017>, 2002.
- 536 Simó, R., Grimalt, J. O., and Albaigés, J.: Dissolved dimethylsulphide, dimethylsulphoniopropionate and  
537 dimethylsulphoxide in western Mediterranean waters, *Deep-Sea Res. Pt II*, 44(3–4), 929–950,  
538 [https://doi.org/10.1016/S0967-0645\(96\)00099-9](https://doi.org/10.1016/S0967-0645(96)00099-9), 1997.
- 539 Staubes, R., and Georgii, H.-W.: Biogenic sulfur compounds in seawater and the atmosphere of the Antarctic region,  
540 *Tellus B*, 45(2), 127–137, <https://doi.org/10.3402/tellusb.v45i2.15587>, 1993.
- 541 Uher, G., and Andreae, M. O.: Photochemical production of carbonyl sulfide in North Sea water: a process study,  
542 *Limnol. Oceanogr.*, 42(3), 432–442, <https://doi.org/10.4319/lo.1997.42.3.0432>, 1997.
- 543 Ulshöfer, V. S., Flöck, O. R., Uher, G., and Andreae, M. O.: Photochemical production and air-sea exchange of  
544 carbonyl sulfide in the eastern Mediterranean Sea, *Mar. Chem.*, 53(53), 25–39, <https://doi.org/10.1016/0304->



- 545 4203(96)00010-2, 1996.
- 546 Ulshöfer, V. S., Uher, G., and Andreae, M. O.: Evidence for a winter sink of atmospheric carbonyl sulfide in the  
547 northeast Atlantic Ocean, *Geophys. Res. Lett.*, 22(19), 2601–2604, <https://doi.org/10.1029/95GL02656>, 1995.
- 548 Wakeham, S. G., Howes, B. L., Dacey, J. W. H., Schwarzenbach, R. P., and Zeyer, J.: Biogeochemistry of  
549 dimethylsulfide in a seasonally stratified coastal salt pond, *Geochim. Cosmochim. Acta.*, 51(6), 1675–1684,  
550 [https://doi.org/10.1016/0016-7037\(87\)90347-4](https://doi.org/10.1016/0016-7037(87)90347-4), 1987.
- 551 Wang, J., Chu, Y.-X., Tian, G., and He, R.: Estimation of sulfur fate and contribution to VSC emissions from lakes  
552 during algae decay, *Sci. Total Environ.*, 856, 159193, <http://dx.doi.org/10.1016/j.scitotenv.2022.159193>, 2023.
- 553 Weiss, P. S., Johnson, J. E., Gammon, R. H., and Bates, T. S.: Reevaluation of the open ocean source of carbonyl  
554 sulfide to the atmosphere, *J. Geophys. Res.-Atmos.*, 100(D11), 23083–23092, <https://doi.org/10.1029/95JD01926>,  
555 1995.
- 556 Whelan, M. E., Lennartz, S. T., Gimeno, T. E., Wehr, R., Wohlfahrt, G., Wang, Y., Kooijmans, L. M. J., Hilton, T.  
557 W., Belviso, S., Peylin, P., Commane, R., Sun, W., Chen, H., Kuai, L., Mammarella, I., Maseyk, K., Berkelhammer,  
558 M., Li, K.-F., Yakir, D., Zumkehr, A., Katayama, Y., Ogée, J., Spielmann, F. M., Kitz, F., Rastogi, B., Kesselmeier,  
559 J., Marshall, J., Erkkilä K.-M., Wingate, L., Meredith, L. K., He, W., Bunk, R., Launois, T., Vesala, T., Schmidt,  
560 J. A., Fichot, C. G., Seibt, U., Saleska, S., Saltzman, E. S., Montzka, S. A., Berry, J. A., and Campbell, J. E.:  
561 Reviews and syntheses: carbonyl sulfide as a multi-scale tracer for carbon and water cycles, *Biogeosciences*, 15,  
562 3625–3657, <https://doi.org/10.5194/bg-15-3625-2018>, 2018.
- 563 Xie, H., Moore, R. M., and Miller, W. L.: Photochemical production of carbon disulphide in seawater, *J. Geophys.*  
564 *Res.-Oceans*, 103(C3), 5635–5644, <https://doi.org/10.1029/97JC02885>, 1998.
- 565 Xu, X., Bingemer, H. G., Georgii, H.-W., Schmidt, U., and Bartell, U.: Measurements of carbonyl sulfide (COS) in  
566 surface seawater and marine air, and estimates of the air-sea flux from observations during two Atlantic cruises, *J.*  
567 *Geophys. Res.-Atmos.*, 106(D4), 3491–3502, <https://doi.org/10.1029/2000JD900571>, 2001.
- 568 Yang, G.-P., Jing, W.-W., Kang, Z.-Q., Zhang, H.-H., and Song, G.-S.: Spatial variations of dimethylsulfide and  
569 dimethylsulfoniopropionate in the surface microlayer and in the subsurface waters of the South China Sea during  
570 springtime, *Mar. Environ. Res.*, 65, 85–97, <https://doi.org/10.1016/j.marenvres.2007.09.002>, 2008.
- 571 Yang, G.-P., Song, Y.-Z., Zhang, H.-H., Li, C.-X., and Wu, G.-W.: Seasonal variation and biogeochemical cycling of



- 572 dimethylsulfide (DMS) and dimethylsulfoniopropionate (DMSP) in the Yellow Sea and Bohai Sea, *J. Geophys.*  
573 *Res.-Oceans*, 119(12), 8897–8915, <https://doi.org/10.1002/2014JC010373>, 2014.
- 574 Yang, G.-P., Zhang, S.-H., Zhang, H.-H., Yang, J., and Liu, C.-Y.: Distribution of biogenic sulfur in the Bohai Sea  
575 and northern Yellow Sea and its contribution to atmospheric sulfate aerosol in the late fall, *Mar. Chem.*, 169, 23–  
576 32, <https://doi.org/10.1016/j.marchem.2014.12.008>, 2015.
- 577 Yu, J., Sun, M.-X., and Yang, G.-P.: Occurrence and emissions of volatile sulfur compounds in the Changjiang estuary  
578 and the adjacent East China Sea, *Mar. Chem.*, 238, 104062, <https://doi.org/10.1016/j.marchem.2021.104062>, 2022.
- 579 Zepp, R. G., and Andreae, M. O.: Factors affecting the photochemical production of carbonyl sulfide in seawater,  
580 *Geophys. Res. Lett.*, 21(25), 2813–2816, <https://doi.org/10.1029/94GL03083>, 1994.
- 581 Zhang, S.-H., Yang, G.-P., Zhang, H.-H., and Yang, J.: Spatial variation of biogenic sulfur in the south Yellow Sea  
582 and the East China Sea during summer and its contribution to atmospheric sulfate aerosol, *Sci. Total Environ.*, 488–  
583 489, 157–167, <https://doi.org/10.1016/j.scitotenv.2014.04.074>, 2014.
- 584 Zhao, Y., Schlundt, C., Booge, D., and Bange, H. W.: A decade of dimethyl sulfide (DMS),  
585 dimethylsulfoniopropionate (DMSP) and dimethyl sulfoxide (DMSO) measurements in the southwestern Baltic Sea,  
586 *Biogeosciences*, 18, 2161–2179, <https://doi.org/10.5194/bg-18-2161-2021>, 2021.
- 587 Zhu, R., Yang, G.-P., and Zhang, H.-H.: Temporal and spatial distributions of carbonyl sulfide, dimethyl sulfide, and  
588 carbon disulfide in seawater and marine atmosphere of the Changjiang Estuary and its adjacent East China Sea,  
589 *Limnol. Oceanogr.*, 64, 632–649, <https://doi.org/10.1002/lno.11065>, 2019.
- 590 Zhu, R., Zhang, H.-H., and Yang, G.-P.: Determination of volatile sulfur compounds in seawater and atmosphere,  
591 *Chin. J. Anal. Chem.*, 45(10), 1504–1510, (in Chinese with English abstract), <https://doi.org/10.11895/j.issn.0253-3820.170291>, 2017.
- 593 Zumkehr, A., Hilton, T. W., Whelan, M., Smith, S., Kuai, L., Worden, J., and Campbell, J. E.: Global gridded  
594 anthropogenic emissions inventory of carbonyl sulfide, *Atmos. Environ.*, 183, 11–19,  
595 <https://doi.org/10.1016/j.atmosenv.2018.03.063>, 2018.
- 596



597 **Figure captions**

598 **Fig. 1.** Sampling stations in the Yellow Sea and Bohai Sea during (a) spring and (b) summer (▲ indicates stations  
599 where atmospheric samples were collected). Yellow Sea Costal Current: YSCC; Changjiang Diluted Water: CDW;  
600 Yellow Sea Cold Water Mass: YSCWM; Yellow Sea Warm Current: YSWC; Taiwan Warm Current: TWC; Kuroshio  
601 Current: KC. The maps were plotted with Ocean Data View (ODV software) (Schlitzer, 2023).

602 **Fig. 2.** Spatial distributions of temperature, salinity, Chl *a*, COS, DMS, CS<sub>2</sub>, and DOC in the surface water of the BS  
603 and YS in spring.

604 **Fig. 3.** Spatial distributions of temperature, salinity, Chl *a*, COS, DMS, CS<sub>2</sub>, and DOC in the surface water of the BS  
605 and YS in summer.

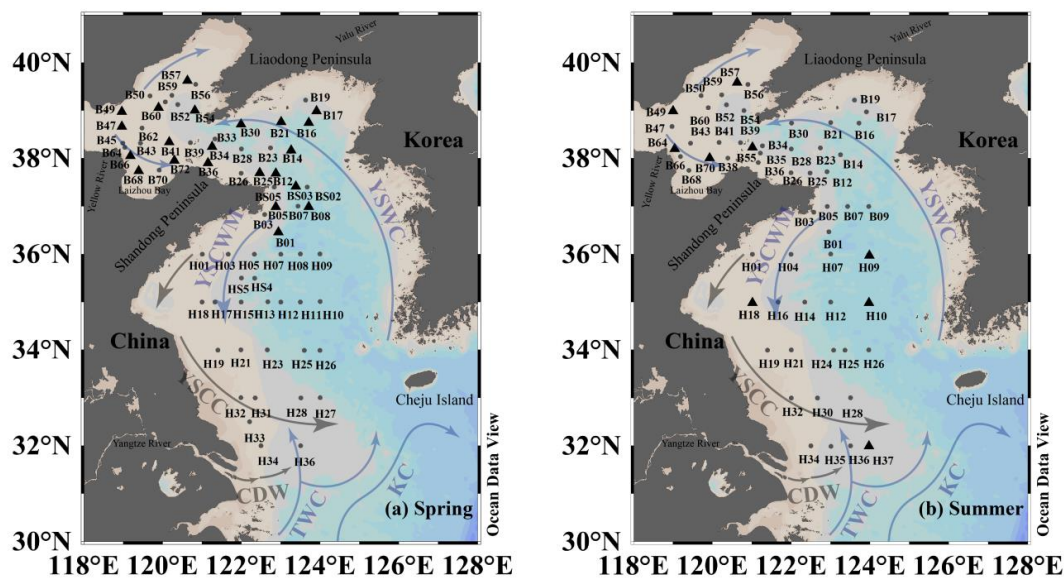
606 **Fig. 4.** Depth distributions of temperature, salinity, Chl *a*, COS, DMS, and CS<sub>2</sub> in seawater in spring.

607 **Fig. 5.** Depth distributions of temperature, salinity, Chl *a*, COS, DMS, and CS<sub>2</sub> in seawater in summer.

608 **Fig. 6.** Spatial distributions of COS, DMS, and CS<sub>2</sub> in the atmosphere over the BS and YS in (a) spring and (b) summer.

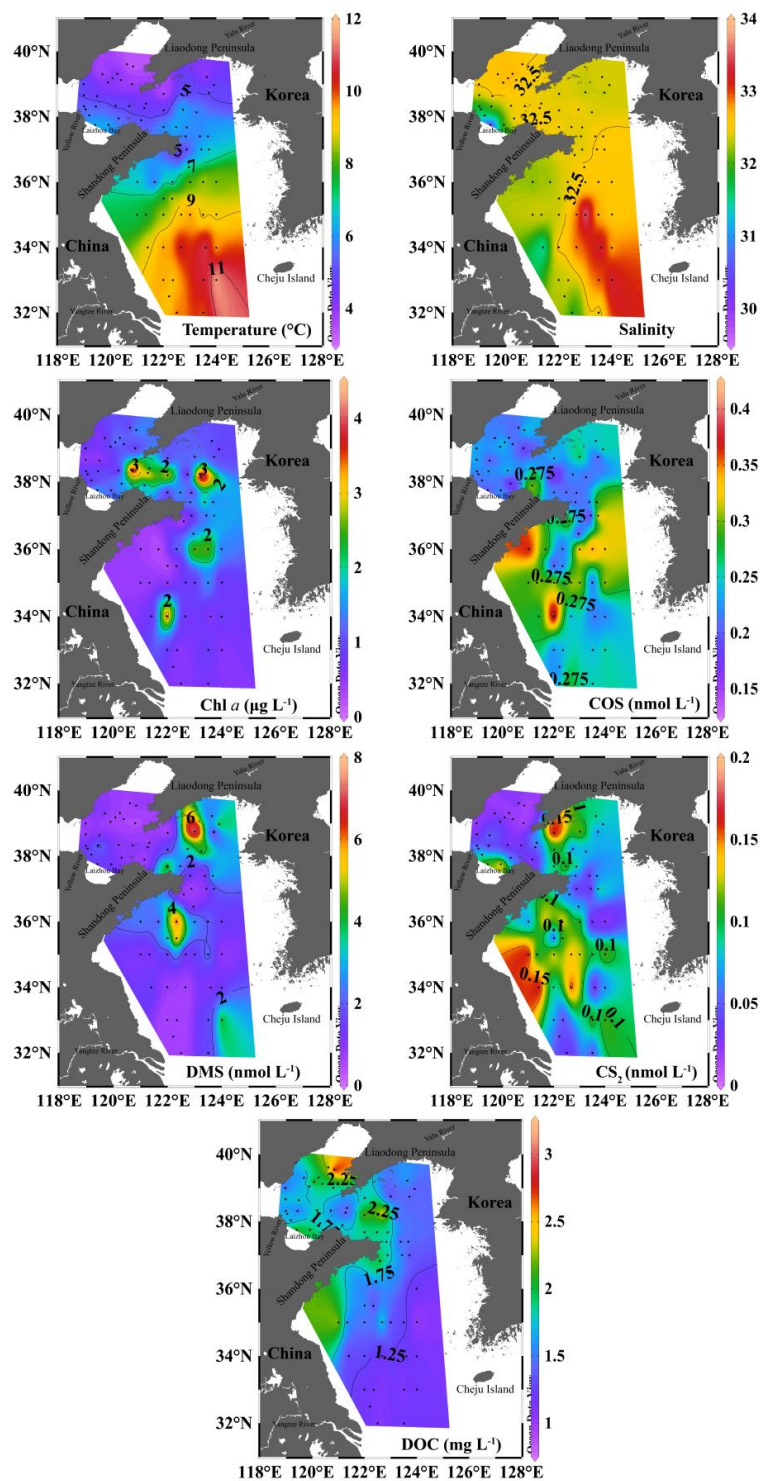
609 **Fig. 7.** Variations of sea-to-air fluxes of VSCs, VSCs concentrations in seawater, and wind speeds in the BS and YS  
610 in spring 2018.

611 **Fig. 8.** Variations of sea-to-air fluxes of VSCs, VSCs concentrations in seawater, and wind speeds in the BS and YS  
612 in summer 2018.



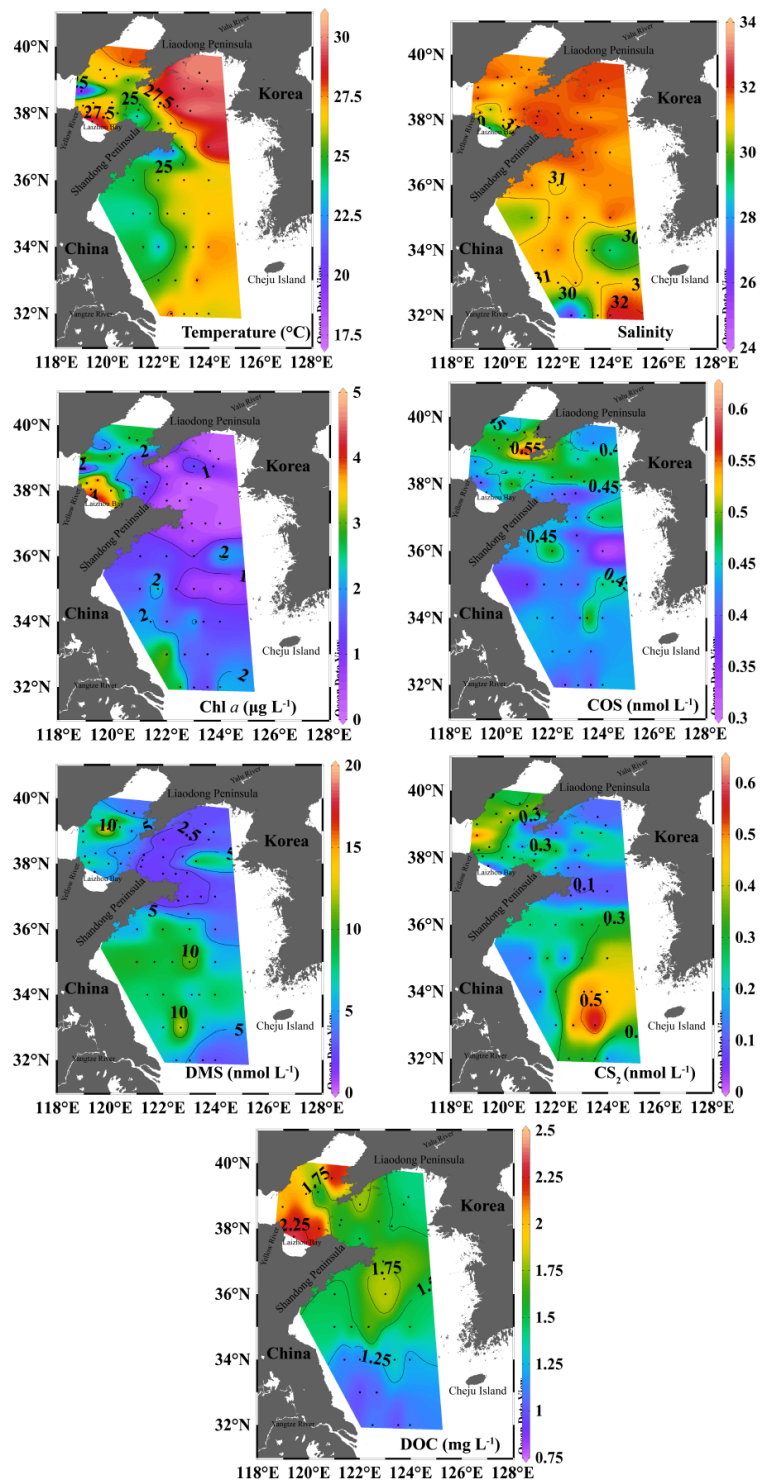
613  
614  
615  
616  
617  
618

**Fig. 1.** Sampling stations in the Yellow Sea and Bohai Sea during (a) spring and (b) summer (▲ indicates stations where atmospheric samples were collected). Yellow Sea Coastal Current: YSCC; Changjiang Diluted Water: CDW; Yellow Sea Cold Water Mass: YSCWM; Yellow Sea Warm Current: YSWC; Taiwan Warm Current: TWC; Kuroshio Current: KC. The maps were plotted with Ocean Data View (ODV software) (Schlitzer, 2023).



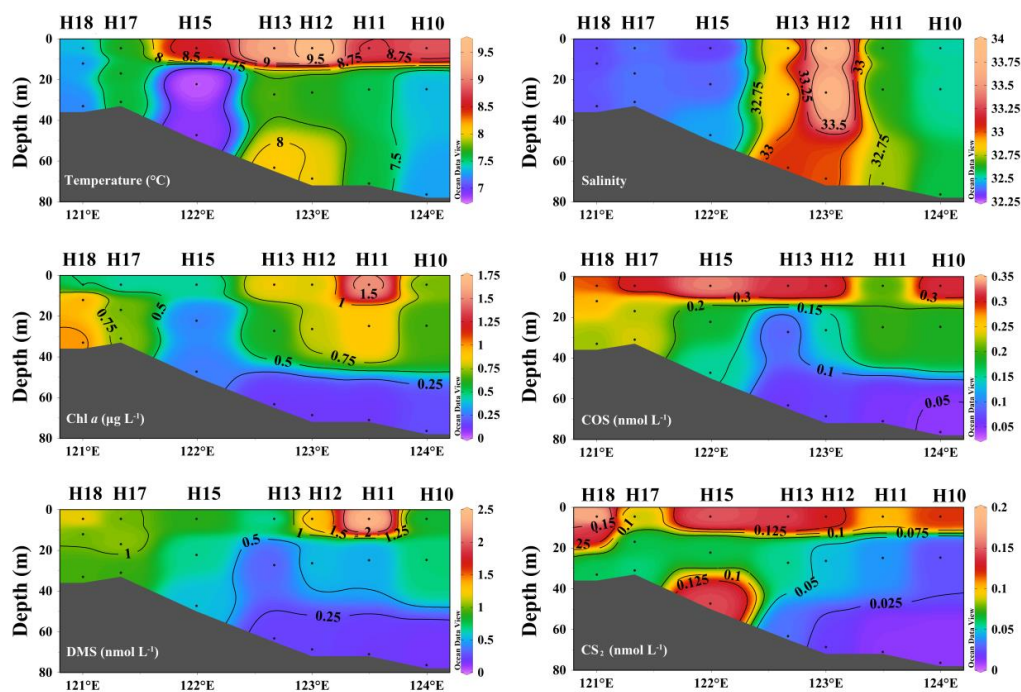


620 **Fig. 2.** Spatial distributions of temperature, salinity, Chl *a*, COS, DMS, CS<sub>2</sub>, and DOC in the surface water of the BS  
621 and YS in spring.



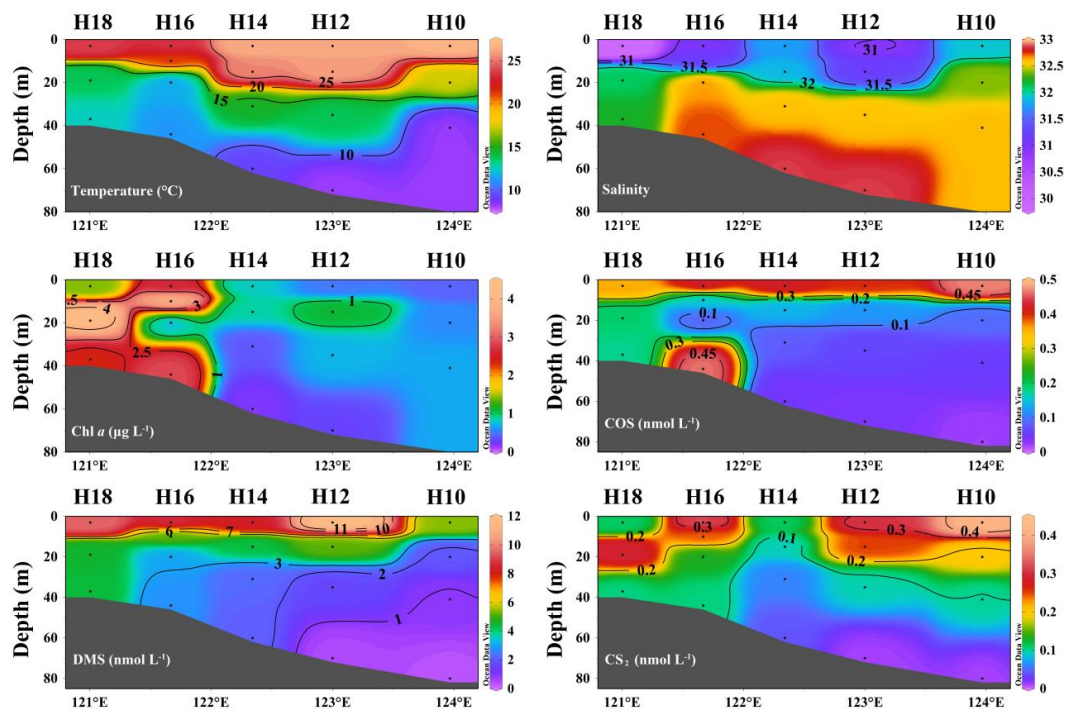


623 **Fig. 3.** Spatial distributions of temperature, salinity, Chl *a*, COS, DMS, CS<sub>2</sub>, and DOC in the surface water of the BS  
624 and YS in summer.



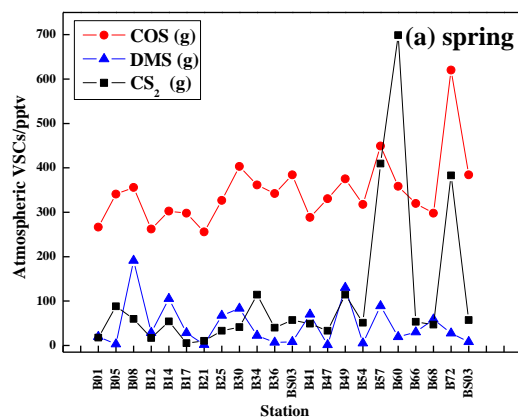
625  
626  
627

**Fig. 4.** Depth distributions of temperature, salinity, Chl *a*, COS, DMS, and CS<sub>2</sub> in seawater in spring.

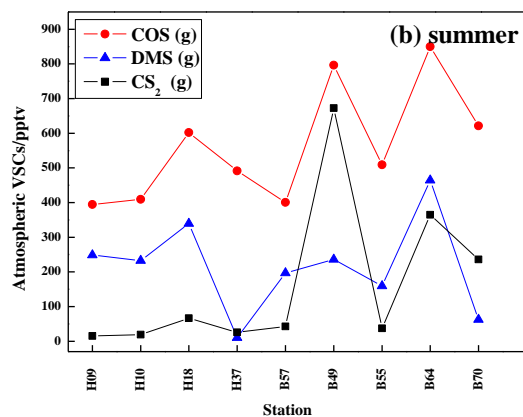


628  
629  
630

**Fig. 5.** Depth distributions of temperature, salinity, Chl *a*, COS, DMS, and CS<sub>2</sub> in seawater in summer.

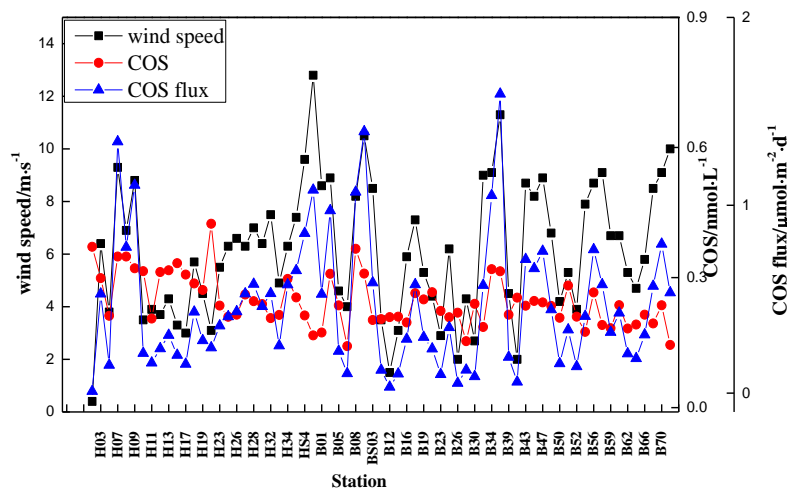


631

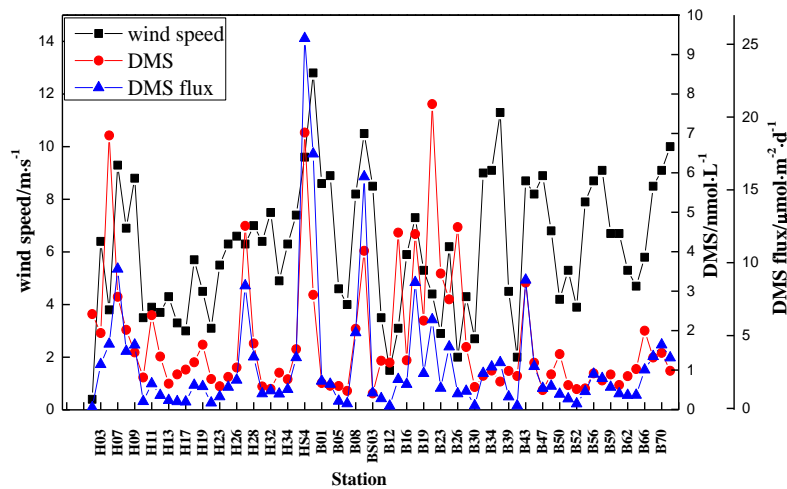


632

633 **Fig. 6.** Spatial distributions of COS, DMS, and CS<sub>2</sub> in the atmosphere over the BS and YS in (a) spring and (b) summer.

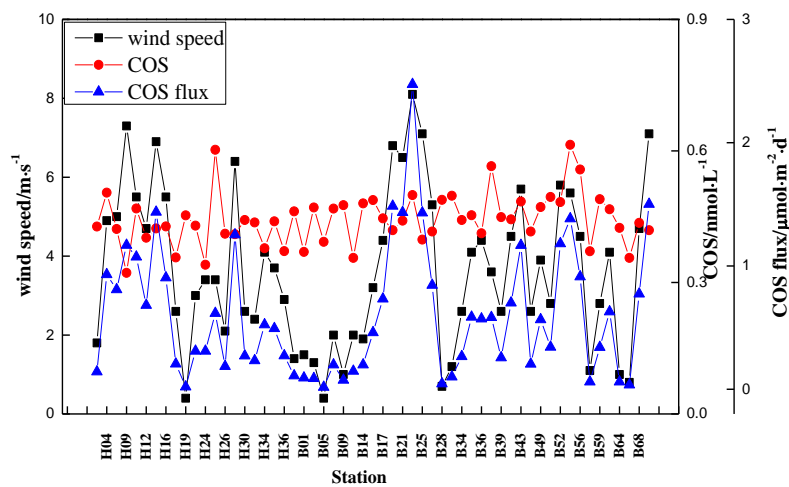


634

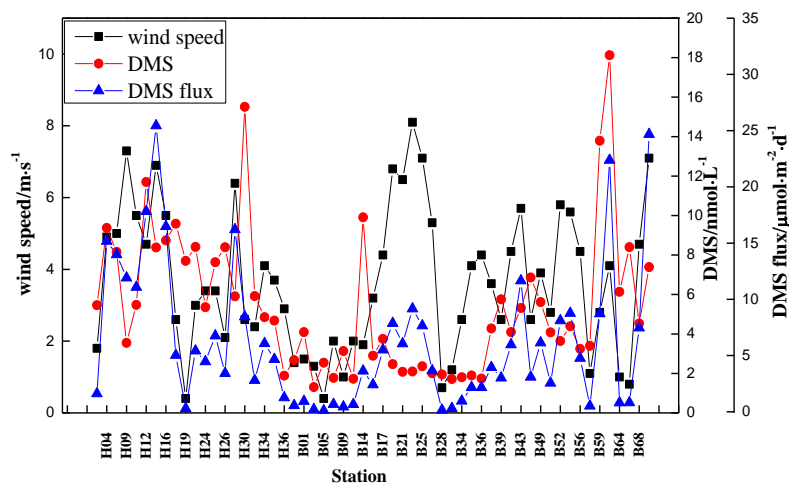


635

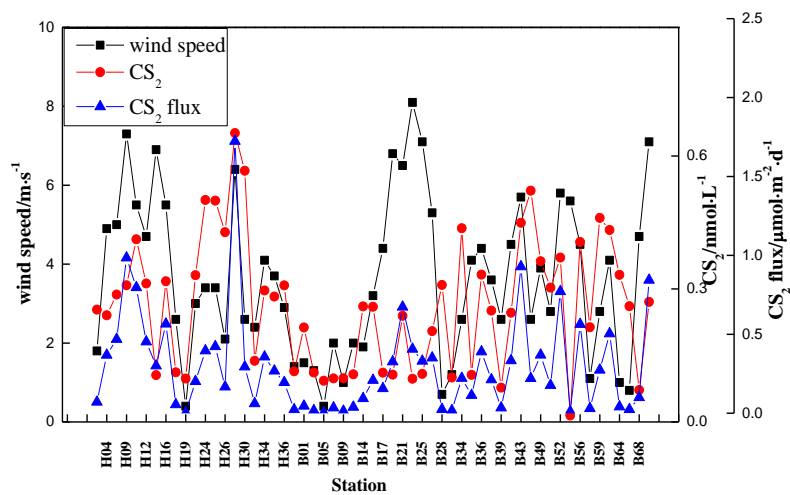




639



640



641

642 **Fig. 8.** Variations of sea-to-air fluxes of VSCs, VSCs concentrations in seawater, and wind speeds in the BS and YS

643

in summer 2018.